Thermal Characterization and Thermal Effect Assessment of Biofouling around a Dynamic Submarine Electrical Cable

Ziad Maksassi, Bertrand Garnier, Ahmed Ould El Moctar, Franck Schoefs, Emmanuel Schaeffer

Thermal Characterization and Thermal Effect Assessment of Biofouling around a Dynamic Submarine Electrical Cable

Ziad Maksassi [1,2,*], Bertrand Garnier [1], Ahmed Ould El Moctar [1], Franck Schoefs [2] and Emmanuel Schaeffer [3]

[1] Nantes Université, Centre National de la Recherche Scientifique (CNRS), Laboratoire de thermique et énergie de Nantes (LTeN), Unité Mixte de Recherche (UMR) 6607, F-44000 Nantes, France; bertrand.garnier@univ-nantes.fr (B.G.); ahmed.ouldelmoctar@univ-nantes.fr (A.O.E.M.)

[2] Nantes Université, École Centrale Nantes, CNRS, Institut de Recherche en Génie Civil et Mécanique (GeM), UMR 618, Institut Universitaire Mer et Littoral (IUML) FR 3473, F-44000 Nantes, France; franck.schoefs@univ-nantes.fr

[3] Nantes Université, Institut de Recherche en Énergie Électrique de Nantes Atlantique (IREENA), Unité de Recherche (UR) 4642, IUML FR 3473, F-44600 Saint-Nazaire, France; emmanuel.schaeffer@univ-nantes.fr

Abstract: Wind energy is expected to play a significant role in meeting emission targets over the next 20 years. Offshore wind turbines in deep water (>150 m) must be developed due to resource quality, environmental, and activity constraints. Floating offshore wind turbines (FOWT) will be the best technology for reaching these targets. The dynamic submarine electrical cable (DSEC) is a key component of FOWT. Its electric insulation system is intended to withstand a maximum conductor temperature of 90 °C. However, biofouling growth, particularly mussels, can modify the heat transfer around the cable and thus its maximum conductor temperature, as well as temperature fluctuation, affecting the fatigue lifetime. In our work we estimate the effective thermal conductivity of mussels of various ages, as well as the heat transfer coefficient of the water around them. The results revealed that the effective thermal conductivity of juvenile mussels is lower than that of mix (both juvenile and adult) and only adult mussels. This variation in effective thermal conductivity with mussel age is related to the water porosity of the mussel's layer. Then, the thermal effect of the resulting global thermal resistance can lead the DSEC conductor wire to either overheat (colonized by juvenile and mixed mussels) or cool down (colonized by adult mussels). Numerical simulations are used to quantify this effect.

Keywords: electric dynamic cable; biofouling; thermal characterization of biofouling; effective thermal conductivity; marine renewable energy; floating offshore wind turbine; mussels

1. Introduction

Sustainable or renewable energy is considered as a primary solution to global warming; it contributes significantly to environmental improvement by reducing CO_2 emissions. One of the most developed renewable energy technologies is the offshore wind turbine (OWT). There are two types of OWT: floating offshore wind turbines (FOWT) and bottom-fixed offshore wind turbines. FOWT is more efficient than bottom-fixed offshore wind turbines and on-land wind turbines because wind speed is higher far from the coast than near the coast, where a small increase in wind yields a large increase in energy production [1]. For example, a turbine with a wind speed of 24 km/h can generate twice as much energy as a turbine with a wind speed of 19 km/h [2]. By increasing the distance to the coast the water depth increases and FOWT are expected to fulfill these requirements for medium (>60 m) [3] or deep water depth (>150 m). Other benefits of installing FOWT over fixed-offshore wind farms include less visual disturbance, noise avoidance (considering the propagation in water of the low frequencies on large distances, this aspect must be carefully analyzed for environmental concerns [4]), stronger and more consistent wind, lower installation costs, no wind turbine size restrictions, and the FOWT is more environmentally friendly [5]. However, FOWT has some drawbacks, such as technical difficulties with mooring lines and power cable design and electrical connections. Furthermore, the distance between the shore and the offshore makes repair and maintenance operations more time consuming and, as a result, more expensive [6]. The transportation of produced energy to shore is a significant challenge for any offshore wind farm. Floating systems require a dynamic cable, which connects the floating hull to the main export cable on the seafloor. According to the experience of floating offshore installations in the oil industry, the greatest stresses are manifested at the head of the cable, that is, at the point of connection with the part fixed to the float. To reduce these stresses, and thus the fatigue of this section of the cable, a bending device with floats and a tensioner is used to shape the section just before the connection into a “s” shape [7]. The technical design of power cable and of electrical connectors are one of the main challenges of the FOWT. The floating offshore wind turbine first sends power to a transformer via an undersea dynamic power cable, and the transformer then sends power to a converter platform via a static power cable. The alternating current is converted to high direct current and sent to a land-based converter station, where it is converted into three phases of electric power. As shown in Figure 1, there are two types of submarine power cable: static cable, which sits on top of or is buried beneath the seafloor, and dynamic cable (or umbilical), which is deployed through the water column between the surface and the seafloor. The movement of the floating platform, as well as wave excitation and currents, all have an impact on this dynamic cable. As a result, while dynamic power cables are an important component of electrical connections, their design, which must account for electrical, mechanical, and thermal concerns, remains a challenge for manufacturers. Any external factor reducing its efficiency will result in lower energy reception.

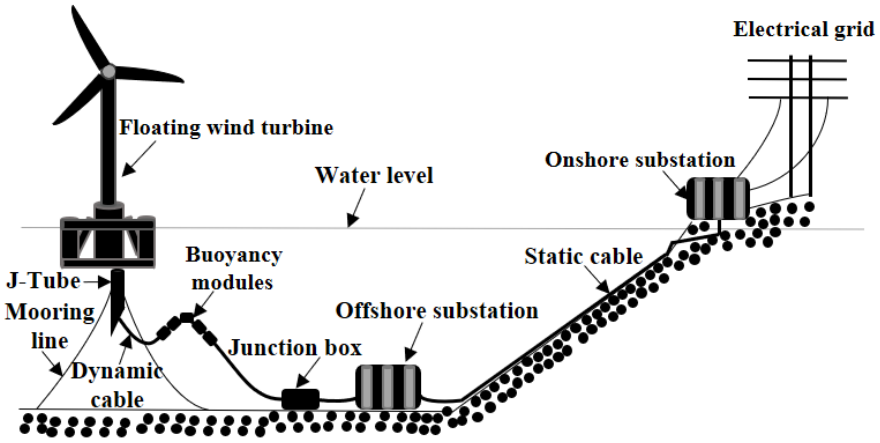

Figure 1. Power transmission system of floating offshore wind turbine.

Biofouling is a complex, dynamic, and a lengthy procedure involving a variety of biological mechanisms that are not fully comprehended [6]. Mollusc bivalves, particularly mussels, are a common and a troublesome fouling element to assemblies related to ship's sea chests and pipework [8,9]. These species have shown to be dominant in coastal Atlantic areas [10–12]. Indeed, biofouling growth, particularly that of mussels (Figure 2), can modify heat transfer around the cable, affecting cable temperature, whereas the cross-linked polyethylene (XLPE) electric insulation system of a dynamic submarine electrical cable (DSEC) is designed to support a maximum copper wire temperature of only 90 °C continuously, according to IEC standard [13]. This maximum conductor temperature is considered a limit to avoid wire insulation (XLPE) degradation.

Figure 2. Juvenile Mussel's colonization (6 months)—Aiguillon sur mer, France, 8 July 2020.

Therefore, it is important to investigate the thermal effect of mussels around the cable in order to determine whether it will affect the heat transfer between cable and water in a positive or negative way. To accomplish this, a thermal characterization of the mussels should be performed, followed by an examination of the effect of mussels biofouling on the temperature of the DSEC copper conductor wire. To our knowledge, there have been no previous studies on the thermal characterization of mussels around cables. The heat transfer coefficient of the water surrounding the mussels, as well as the "effective" thermal conductivity of different mussel age classes (juvenile (six-month-old), mixed (juveniles and adults), and adults (12-month-old) [14], are measured in this study. In addition, numerical simulations of temperature field of DSEC colonized with mussels of various ages are performed. In the following section the experimental measurement of the effective thermal conductivity of various ages of mussels and the heat transfer coefficient of the water around them for uniform and non-uniform colonization will be presented.

2. Thermal Characterization of Mussels

The effective thermal conductivity of the mussels is calculated using a 1D analytical stationary model (Fourier's law) that assumes the mussels are distributed uniformly around the tube. The measurement method is validated by comparing the thermal conductivity of a double-sided foam adhesive to that of a hot guarded plate device. In addition, Newton's law is used to calculate the heat transfer coefficient of the water surrounding the mussels. It is also compared to two literature correlations [15]. Furthermore, non-uniform distributions of mussels around the tube were taken into account; in practice, mussel growth occurs undersea primarily on the tops of horizontal electric cables because

light comes from above. In this case, due to more complicated geometry, the effective thermal conductivity of mussels of different ages and the heat transfer coefficient of the water around the mussels are estimated using a numerical method (finite elements via COMSOL) to solve the 2D heat transfer equation and a parameter estimation technique (the simplex method).

2.1. Experimental Setup and Mussel's Samples

The stationary measurements are carried out using an experimental tube as shown in Figure 3. It consists of an aluminum tube (ϕ_{int} = 60 mm, ϕ_{ext} = 70 mm, L = 600 mm) implemented with 5 K-type thermocouples (three in the middle cross section with 120° angle and one thermocouple on each of the two other cross-sections close to the extremities of the tube (at 5 cm). On the inner side of the aluminum tube, six silicon rubber resistance tapes (L = 600 cm, w = 25.4 mm) with copper etched foil (SRFGA-124/2-P from Omega) are used to provide uniform heating. A rubber air chamber with an internal pressure of about 1.5 bar keeps the six heaters in contact with the aluminum tube and provides adiabatic boundary conditions inside the aluminum tube.

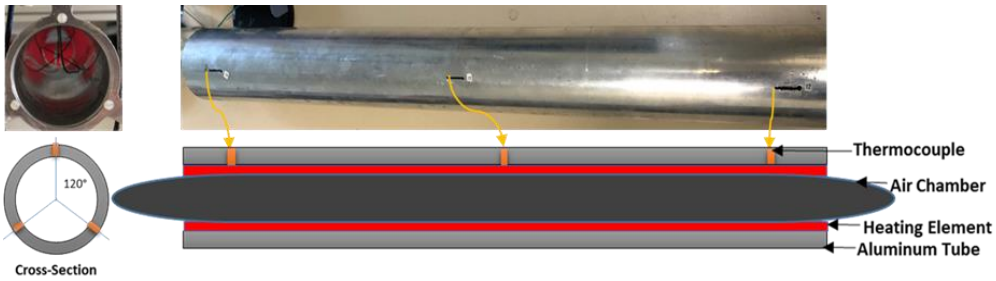

Figure 3. Schematic for the experimental tube.

Furthermore, a sample holder is manufactured to allow measurement inside a tank filled with immobile sea water. As shown in Figure 4, the aluminum tube's supporting system consists of a POM (polyoxymethylene) seal secured to each end of the tube with a plastic screw, carried up by a U-clamp connected to a T-shaped support.

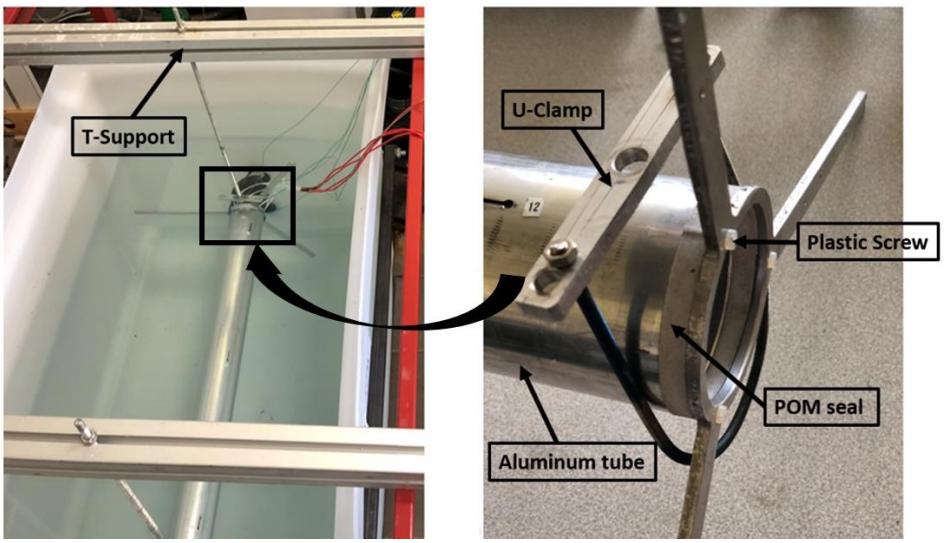

Figure 4. Experimental tube support.

Just prior to the measurement, different age classes of mussels, juvenile, mix and adult, as shown in Figure 5a, 5b and 5c, respectively, are spread around the experimental tube consecutively and maintained using a steel net (1 cm mesh), as shown in Figure 6.

Figure 5. Different ages of mussels: (**a**) Juvenile, (**b**) mix (juvenile and adult) and (**c**) adult.

Figure 6. Uniform distribution of mussels around the experimental tube held by a steel net.

One should note that these mussels were extracted from the Atlantic Ocean at the mussel breeding site (Aiguillon sur Mer, France, 8 July 2020). Patches of size 30 cm × 20 cm are collected from the lines (Figure 2) in view of rebuilding a colonization with the same organization of the species as the on site conditions. All thermal property measurements of mussels were performed within 24 h after their withdrawal from the sea in order to keep the mussels alive. The shells were closed during the entire test. During the measurement campaign, the limited time available to prepare the samples and perform all of the steady-state measurements was a significant constraint.

2.2. Thermal Characterization for a Uniform Colonization of Mussels around the Tube

In this section, different ages of mussels were thermally characterized by fixing them with a uniform colonization shape around the experimental tube, which means that the entire experimental tube is covered with mussels of the same thickness.

2.2.1. Measurement Method

During the experiment, the instrumented aluminum tube is immersed in a tank of sea water, and the power provided by the heating elements inside the tube is used to achieve a steady state temperature with a temperature difference of about 4 K to 10 K between both sides of the mussel layer. Fourier's law is directly used to calculate the effective thermal conductivity of mussels in the case of uniform colonization (100 percent coverage of mussels around the tube), and this is done using the temperature difference between the two sides of the mussel layer and the power of the mussel layer Q (W) crossing it (Equation (1)). In addition, the heat transfer coefficient between the mussel layer and external water is found from the expression of a Robin boundary condition (Equation (2)). Therefore, the computation of the effective thermal conductivity of mussels k_{biof} ($W.m^{-1}.K^{-1}$) and of the heat

transfer coefficient of water h_w (W.m^{-2}.K^{-1}) around the mussels for an uniform colonization, as shown in Figure 7, is represented by the following Equations (1) and (2), respectively:

$$k_{biof} = \frac{ln\left(\frac{r_e}{r_i}\right).Q}{2\pi.L.(T_{av1}-T_{av2})} \quad (1)$$

$$h_w = \frac{Q}{2\pi.r_e.L.(T_{av2}-T_w)} \quad (2)$$

where T_{av1} is the average temperature on the internal side of the mussel layer (average of T_1 *(K)*, T_2 *(K)* and T_3 *(K)*) measured by the three thermocouples in the middle cross-section and located in the aluminum tube. T_{av2} *(K)* is the average temperature on the external side of the mussel layer (average of T_4 *(K)*, T_5 *(K)* and T_6 *(K)*) and T_w *(K)* is the temperature of the water far away from the aluminum tube. In Equations (1) and (2), r_i and r_e are respectively the internal and external radius of the mussel layer and *L* is its length. This radial conductivity relation applied in the case of negligible axial heat loss will be tested later.

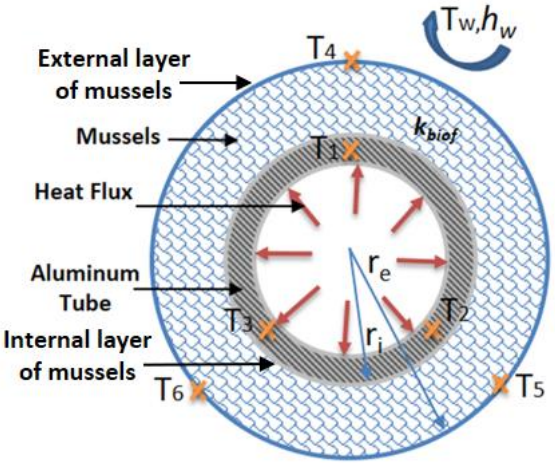

Figure 7. Middle cross-section of the aluminum tube with uniform mussels colonization.

Noting that, in accordance to the law of the propagation of uncertainties [16], the absolute uncertainty on the effective thermal conductivity of mussels is obtained by:

$$\delta k = \sqrt{\left(\frac{dk}{dL}\delta L\right)^2 + \left(\frac{dk}{dT_{av1}}\delta T_{av1}\right)^2 + \left(\frac{dk}{dT_{av2}}\delta T_{av2}\right)^2 + \left(\frac{dk}{dU}\delta U\right)^2 + \left(\frac{dk}{dI}\delta I\right)^2 + \left(\frac{dk}{dr_i}\delta r_i\right)^2 + \left(\frac{dk}{dr_e}\delta r_e\right)^2} \quad (3)$$

where *U* and *I* are respectively the measured voltage and current through the heating element (*Q* = *U.I*) it follows then:

$$\delta k = \sqrt{\begin{array}{l}\left(\frac{-\ln\left(\frac{re}{ri}\right)*U*I}{2\pi L^2(T_{av2}-T_{av1})}\delta L\right)^2 + \left(\frac{\ln\left(\frac{re}{ri}\right)*U*I}{2\pi L(T_{av2}-T_{av1})^2}\delta T_{av1}\right)^2 + \left(\frac{-\ln\left(\frac{re}{ri}\right)*U*I}{2\pi L(T_{av2}-T_{av1})^2}\delta T_{av2}\right)^2 \\ + \left(\frac{\ln\left(\frac{re}{ri}\right)*I}{2\pi L(T_{av2}-T_{av1})}\delta U\right)^2 + \left(\frac{\ln\left(\frac{re}{ri}\right)*U}{2\pi L(T_{av2}-T_{av1})}\delta I\right)^2 + \left(\frac{-U*I}{2\pi L r_i(T_{av2}-T_{av1})}\delta r_i\right)^2 \\ + \left(\frac{U*I}{2\pi L re(T_{av2}-T_{av1})}\delta r_e\right)^2\end{array}} \quad (4)$$

Also, the uncertainties on the heat transfer coefficient h_w is calculated similarly to the one of thermal conductivity.

The thermal characterization method and experimental setup were tested with a material double sided tape adhesive (Figure 8a), and thermal conductivity was initially measured with a hot guarded plate (HGP) device (Figure 8b) with a 5% relative uncertainty. The result shows that the thermal conductivity computed using Equation (1) and measured with our experimental setup with aluminum tube was 0.052 $W.m^{-1}.K^{-1}$ (for double sided tape adhesive not covered with steel net) and 0.053 $W.m^{-1}.K^{-1}$ (for double sided tape adhesive covered with steel net), with only a 5.45 percent and 3.64 percent relative discrepancy, respectively. This validation confirms that the steel net (used to maintain the mussels) has no significant effect on the effective thermal conductivity value. It also confirms that the tube extremities connected to the sample holder are thermally well insulated. In other words, the axial heat flux along the aluminum tube is negligible in comparison to the radial one, which explains why the direction along the tube length is ignored in our thermal models (analytical and numerical).

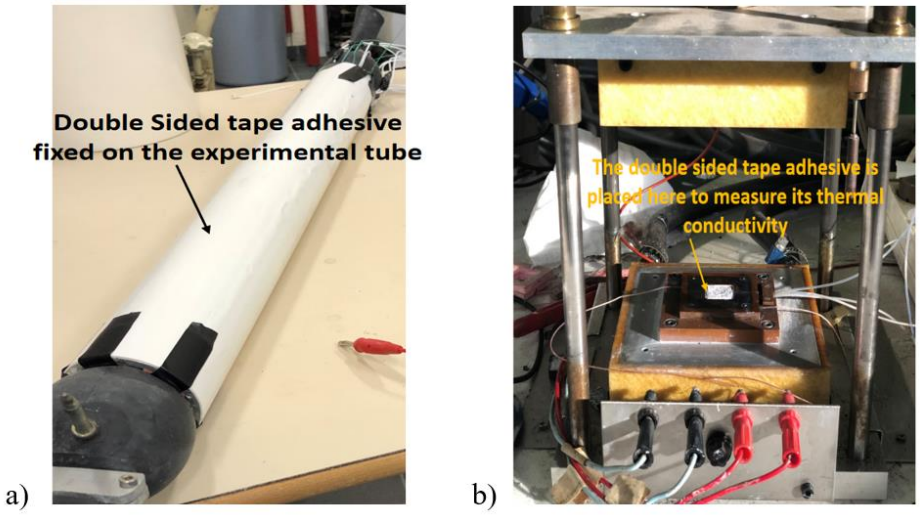

Figure 8. Double adhesive tape on (**a**) experimental tube (**b**) hot guarded plate.

2.2.2. Effective Thermal Conductivity Measurement Results

Table 1 presents the evolution of the mean temperature along the aluminum tube in the presence of mussels for different ages and thicknesses uniformly distributed. It should be noted that the thicknesses of mussel layers are measured just after mussel sample implementation around the tube, yielding 40 mm for juvenile, 60 mm for mix and 70 mm for adult mussels. These thickness values are in agreement with the thicknesses of juvenile and adult mussels from a previous work from SIEVERS [8] (≈50 mm and ≈68 mm respectively).

Mussels Type	T_1	T_2	T_3	T_4	T_5	T_6	T_w	r_i	r_e	Q
	°C	**°C**	**°C**	**°C**	**°C**	**°C**	**°C**	**mm**	**mm**	***W***
Juvenile	35.7	32.82	31.39	23.56	23.1	23.13	23	35	75	228.03
Mix (juvenile and adult)	27.28	26.72	26.6	23.47	22.32	22.31	22.3	35	95	127.75

Adult	28.77	27.9	28.28	23.62	23.52	23.52	23.36	35	105	211.63

Table 1. Distribution of measured temperature around the aluminum tube for different ages of mussels uniformly distributed.

Therefore, the measured values of the effective thermal conductivity of juvenile, mix (juvenile and adult) and adult mussels are 4.4, 8, 12.8 $W.m^{-1}.K^{-1}$, respectively, for a uniform distribution of mussels around the aluminum tube, as shown in Table 2. As the relative uncertainty on k_{biof} measurement is less than 9%, the differences between the various types of colonization is significant.

Table 2. Measured effective thermal conductivities of mussels of various ages uniformly distributed around the aluminum tube.

Mussels Type	k_{biof}	**Absolute Uncertainty**	**Relative Uncertainty**
	$W.m^{-1}.K^{-1}$	**$W.m^{-1}.K^{-1}$**	**%**
Juvenile	4.4	±0.4	9
Mix (juvenile and adult)	8.0	±0.52	6.5
Adult	12.8	±0.97	7.6

One explanation for these discrepancies could be the increasing volume of mussels with age (Figure 5). Indeed, the water porosities of the three biofouling materials increase with mussel age due to differences in mussel size. Therefore, one can expect more natural convection inside older biofouling (in mussel's pore space), resulting in a higher effective thermal conductivity. In order to confirm this assumption, the effect of water circulation in the open pores of a porous media on effective thermal conductivity was investigated. For this purpose, a cluster of glass beads ($\phi_{ext,g}$ = 16 mm) was implemented around the experimental tube and maintained using a steel net, as shown in Figure 9a. Glass medium beads have a water porosity of about 43% and a measured effective thermal conductivity of 2.4 $W.m^{-1}.K^{-1}$, which is higher than the thermal conductivity of water (0.6 $W.m^{-1}.K^{-1}$) and the glass itself (1.1 $W.m^{-1}.K^{-1}$). This shows that there is little water circulation in the porous space, resulting in a higher effective thermal conductivity. In addition, after the glass medium has been covered with a polyethylene stretch film, as shown in Figure 9b, a test is performed. The effective thermal conductivity of the medium glass beads then drops to 2.19 $W.m^{-1}.K^{-1}$, with a discrepancy of less than 9%. Subsequently, the external water has little effect on the effective thermal conductivity of the porous medium.

Figure 9. Experimental tube covered with glass beads (**a**) without plastic cover (**b**) with plastic cover.

Moreover, the homogeneous effective thermal conductivity of glass beads due to Maxwell expression [17] gives a value of 0.85 $W.m^{-1}.K^{-1}$ which is lower than the measured effective thermal conductivity of the glass porous medium, which is 2.4 $W.m^{-1}.K^{-1}$. It should be noted that Maxwell's homogeneous thermal conductivity is valid for large water porosity bigger than 75%, which is bigger than our glass medium's water porosity of 43 percent; however, it gives an idea about the value of the equivalent conductivity of porous media. Therefore, the hypothesis of a small circulation of water due to free convection in the porous space resulting in a higher effective thermal conductivity appears to be the most likely.

2.2.3. Heat Transfer Coefficient of the Water around the Mussels Measurement Results

For a uniform distribution of mussels around the tube, the measured heat transfer coefficients for juvenile, mix (juvenile and adult), and adult mussels, respectively, are 3395, 873, and 2682 $W.m^{-2}.K^{-1}$, as shown in Table 3. However, because the position of the external thermocouple is not very precise (less than 5 mm), and the temperature difference between the mussel's external layer and the water is very small (less than 0.4 °C), the relative uncertainty reaches 19–37 percent. The measured global resistance, however, is unaffected by this relatively high uncertainty.

Table 3. Heat transfer coefficient of the water around the mussels as measured experimentally.

Mussels Type	h_w	Absolute Uncertainty	Relative Uncertainty	$\Delta T_{m,w}$	Absolute Uncertainty	Relative Uncertainty
	$W.m^{-2}.K^{-1}$	$W.m^{-2}.K^{-1}$	%	°C	°C	%
Juvenile	3395	±1123	33	0.23	±0.07	30
Mix (juvenile & adult)	873	±164	19	0.4	±0.07	17.5
Adult	2682	±1003	37	0.2	±0.07	35

$\Delta T_{m,w}$: is the temperature difference between the external layer of mussels and the water.

Furthermore, the analytical stationary method for estimating the heat transfer coefficient of the water around the mussels is validated by comparing the result of the heat transfer coefficient of the water around a tube without the mussels and two literature correlations (Churchill & Chu and Morgan [15]). Table 4 shows that the discrepancy between the experimental value h_w and the one provided by Morgan correlation is equal to 6%, which is less than the discrepancy value of 29% provided by Churchill & Chu's correlation. This is due to the fact that Churchill & Chu's correlation was set for a wide range of Rayleigh number ($R_{aD} \leq 10^{12}$), whereas Morgan's correlation is related to a narrow range of Rayleigh number (Table 9.1 in [15]). Moreover, the heat transfer coefficients obtained from the correlations were applied for an isothermal horizontal cylinder, whereas in our case the experimental tube is not completely isothermal. As a result, the difference between experimental and theoretical correlation values is acceptable.

Table 4. Experimental and theoretical values of the heat transfer coefficient of the water around the experimental tube without mussels.

h_w (Experimental)	h_w (Churchill Chu)	h_w Discrepancy &(Experimental and Churchill & Chu)	h_w (Morgan)	h_w Discrepancy (Experimental and Morgan)
$W.m^{-2}.K^{-1}$	$W.m^{-2}.K^{-1}$	%	$W.m^{-2}.K^{-1}$	%
220	309	29	234	6

Considering the relatively high value of convective heat transfer of water around the mussels, its contribution to overall thermal resistance between the cable and the external water is small when compared to that of biofouling (effective conductive resistance of mussels). In Table 5, we show that the convective resistance of water around juvenile, mix, and adult mussels is 2.2%, 8.3%, and 4.3% of the overall thermal resistance, respectively. As far as natural convection is involved in the porous medium, one can compare its effect to the one of the natural convection in water around the tube without mussels. This can provide an indication of the expected effect of biofouling on the temperature distribution in an electrical cable, as investigated in the final section of this paper. Table 5 shows that the effective conductive resistance of juvenile mussels (0.045 $K.W^{-1}$) is higher than the convective resistance around the tube in the absence of mussels (0.03 $K.W^{-1}$), but it is slightly higher for mix mussels (0.033 $K.W^{-1}$) and smaller for adult mussels (0.022 $K.W^{-1}$). However, in practice, the configuration changes as the composition and thickness of the deposit changes over time during

successive seasons of mussel growth. In this case, we can anticipate that the higher thermal resistance associated with the increased deposit will eventually prevail, resulting in a situation in which the tube is more thermally insulated, causing overheating of the electric cable, which will be detrimental to its service life.

Table 5. Comparison between conductive and convective thermal resistances as a function of the ages of the mussels.

Mussels Type	$R_{conductive(biof)}$	$R_{convective}$	$R_{overall}$	$R_{without(biof)}$	***Effective Conductive Resistance Contribution***	***External Convective Resistance Contribution***
	$K.W^{-1}$	**$K.W^{-1}$**	**$K.W^{-1}$**	**$K.W^{-1}$**	**%**	**%**
Juvenile	0.045	0.001	0.046	0.03	97.8	2.2
Mix (juvenile and adult)	0.033	0.003	0.036		91.7	8.3
Adult	0.022	0.0009	0.023		95.7	4.3

$R_{conductive\ (biof)}$ is the effective conductive thermal resistance of mussels. * $R_{convective}$ is the convective thermal resistance of the water around the mussels. * $R_{overall}$ is the overall thermal resistance of the presence of mussels around the tube (including $R_{conductive(biof)}$ *and* $R_{convective}$). * $R_{without(biof)}$ is the overall thermal resistance without the presence of the mussels.

2.3. Thermal Characterization of a Non-Uniform Colonization of Biofouling around the Tube

Mussels do not grow uniformly around submarine cables in real offshore installations. One reason for this is the sun's non-uniform irradiation. Such a situation with non-uniform biofouling growth around a horizontal tube should also be investigated. As a result, the effective thermal conductivity of the non-uniform mussel distribution around the tube, as well as the heat transfer coefficient of the water around them, were measured. Table 6 shows the measured temperature distribution around a polyethylene covered aluminum tube for different configurations of juvenile mussel colonization distribution (25%, 50% and 100%), as shown in Figure 10.

Table 6. Distribution of measured temperatures around a polyethylene covered aluminum tube colonized by juvenile mussels with different configurations of colonization.

Juvenile Mussels Colonization	T_1	T_2	T_3	T_4	T_5	T_6	T_w	r_i	r_e	Q
%	**°C**	**°C**	**°C**	**°C**	**°C**	**°C**	**°C**	**mm**	**mm**	**W**
25	28.12	26.44	24.8	22.55	-	-	22.3	38.9	78.9	66.33
50	30.82	28.5	26	22.92	-	-	22.45	38.9	78.9	85.43
100	29.48	28.46	28.95	23.03	22.6	22.4	22.12	38.9	78.9	40.74

In the absence of an analytical model to calculate the effective thermal conductivity from measurements in the case of the non-uniform distribution of mussels, a numerical tool will be used for inverse analysis. For this purpose, the effective thermal conductivity of the mussels and the heat

transfer coefficient of the water around the mussels are estimated using a 2D steady state thermal model computed using finite elements (COMSOL software), with the following heat conduction equation:

$$div\left(-k\vec{\nabla}T\right) = 0 \tag{5}$$

where k is the thermal conductivity ($W.m^{-1}.K^{-1}$), T is the absolute temperature (K). The Equation (5) is solved numerically with the associated boundary conditions: imposed heat flux ϕ ($W.m^{-2}$) with $\phi = Q/2\pi r_0 L$ at the inner surface of the aluminum tube and convective heat transfer coefficient (h_{w1} and h_{w2}) at the external surface, as shown in Figure 10.

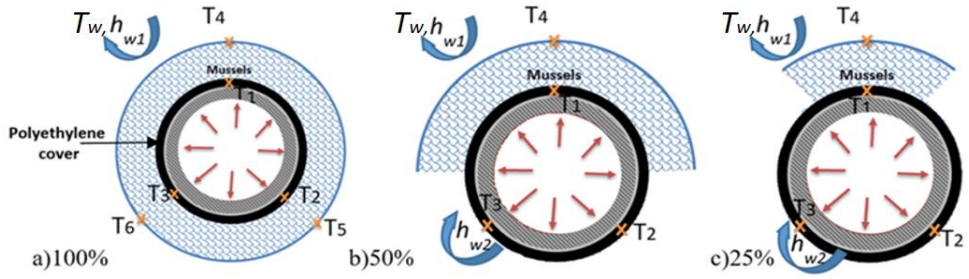

Figure 10. Various colonization distribution configurations around the heated covered polyethylene aluminum tube. (a) 100% colonization, (b) 50 % colonization and (c) 25% colonization.

Where, T_w is the temperature of the surrounding water, h_{w1} and h_{w2} is the heat transfer coefficient of the water around the mussels and the tube, respectively. T_1,T_2,T_3 are the temperatures of surface of the experimental tube. T_4,T_5,T_6 are the temperature of the external layer of mussels.

In the biofouling region, a mesh with 2000 to 5000 nodes was used, while in the aluminum tube region, a mesh with 1000 nodes was used. As shown in Figure 11, the fine mesh type is used.

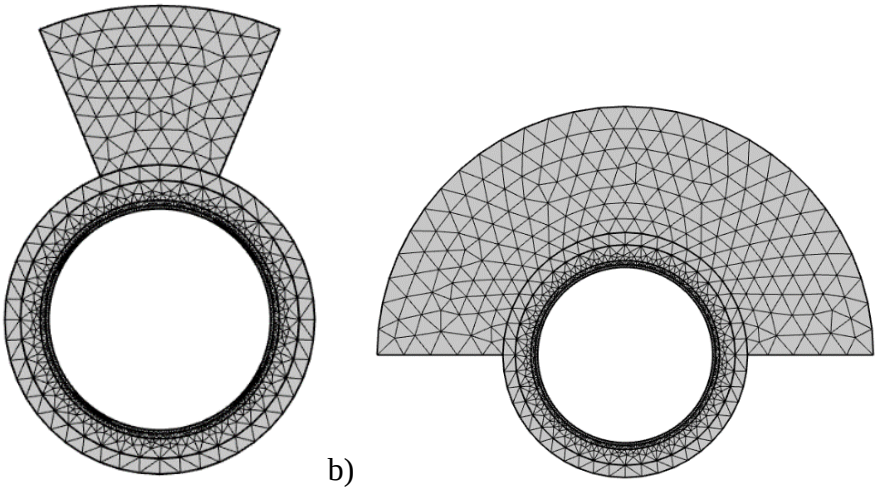

Figure 11. Fine mesh in COMSOL for (**a**) 25% (**b**) 50% mussel colonization.

A robust minimization technique (simplex method) is used to estimate the effective thermal conductivity of mussels from inverse analysis in order to minimize the sum of squares of the difference between measured and calculated temperatures, the latter depending on the three parameter values k_{biof}, h_{w1} and h_{w2}:

$$J = \Sigma_{i=1}^{N} \left(T_{i,calc.}\left(k_{biof}, h_{w1}, h_{w2}\right) - T_{i,meas.}\right)^2 \tag{6}$$

where two different heat transfer coefficients are defined: h_{w1} between biofouling and water and h_{w2} between polyethylene and water. Three different configurations of the distribution of the biofouling (25%, 50% and 100%) around the tube were considered as shown in Figure 10.

In the 2D thermal model, the external temperature of the system is the one of the water and the heat rate of power source is provided by the voltage and current measurements on the heating elements. Table 7 shows the heat transfer coefficient of the water around the mussels with non-uniform colonization around the aluminum tube covered in polyethylene, as well as the estimated effective thermal conductivity of juvenile mussels. The effective thermal conductivity of juvenile mussels for 100% colonization differs from the value obtained previously with an experimental aluminum tube (4.4 $W.m^{-1}.K^{-1}$) and the one obtained here with an aluminum tube covered with a polyethylene layer (1.6 $W.m^{-1}.K^{-1}$). This difference is mainly due to the fact that the temperature gradient between the external and internal radiuses of the mussel layer is not the same in both cases (10 K for aluminum tube and 6 K for aluminum tube covered with polyethylene). That means that convection in the porous medium will not be the same involving different effective thermal conductivities.

Table 7. Effective thermal conductivity of juvenile mussels and heat transfer coefficient of water around the mussels for different percentage of colonization.

Juvenile Mussels Colonization	k_{biof}	**Sensitivity for** k_{biof}	h_{w1}	**Sensitivity for** h_{w1}	h_{w2}	**Sensitivity for** h_{w2}
%	**$W.m^{-1}.K^{-1}$ °C**		**$W.m^{-2}.K^{-1}$ °C**		**$W.m^{-2}.K^{-1}$ °C**	
25	1.4	1	1510	0.1	1960	0.9
50	1.9	1	310	0.1	3910	0.88
100	1.6	5	910	0.1	-	-

The results in Table 7 show that the effective thermal conductivity of uniform (100%) and non-uniform (25% and 50%) colonization is roughly of the same order of magnitude. The difference can be attributed to measurement accuracy and the temperature gradient between the external and internal layers of mussels, which is not exactly the same for the three different configurations.

As in the previous section, the convective coefficient values are relatively high and show some disparity. We have already seen that this parameter has a minor impact on global resistance. In the addition of the values of convective coefficients, Table 7 also shows the sensitivity of the measured temperature to these parameters defined by $\beta\, dT/d\beta$, where β is the parameter (k_{biof}, h_{w1} or h_{w2}). It can be noted that the sensitivity value to the heat transfer coefficients are small compared to the one for the effective thermal conductivity. Because of the convective coefficient's low sensitivity and low contribution to global thermal resistance, its discrepancy has a minor impact on determining the effective thermal conductivity of mussels. The water in our current study is stagnant. However, if there is a current flow velocity of water in the system in a real-world application, then the effect of the global heat transfer coefficient of the water around the cable and in the mussel's layer (porous medium) must be considered.

3. Thermal Effect of Mussels on the DSEC Copper Wire

In Section 2, we demonstrated that the age of the mussels changes the water porosity of the biocolonization, thus affecting the global thermal resistance. It was shown that thermal resistance of a layer of mussels can be lower or higher than convective resistance without mussels. It might be interesting to analyze the effect of colonization on temperature distribution in a real submarine power

cable. Indeed, as described in Section 2.2.3, the effective conductive resistance of juvenile mussels is higher than the convective resistance around the tube in the absence of mussels; however, the effective conductive resistance of mixed mussels is slightly bigger and the effective conductive resistance of adult mussels is slightly lower. Thus, mussel deposits on the surface of the marine power cable can form an insulating layer, resulting in increased thermal resistance. In this section, an analytical model based on an international standard is used to calculate the permissible current rating for a given operating temperature. This yields a power that can be imposed in a 2D numerical simulation model (finite elements via COMSOL) to investigate the thermal effect of different ages of mussels on the temperature of the DSEC copper wire.

3.1. Analytical Model Based on IEC Standard

Under steady-state conditions, IEC standards 60287-1-1 [13] and 60287-2-1 [18] are used to calculate the permissible current rating in accordance with operating temperature. It denotes a constant current load (100 percent load factor) that is only sufficient to generate the maximum conductor temperature asymptotically and assumes that the conditions in the surrounding ambient are constant. This method is widely used all over the world. It covers medium to high voltage cables, a wide range of installation methods, and a formula for current rating and losses. The main goal is to determine the relationship between the cable and the factors influencing heat dissipation, such as the thermal resistance of cable components, load, and the surrounding environment. For illustrating the method, we use a cable for which data were available: a 20 kV cable used in OMDYN2 project. It's a cross-linked polyethylene insulated dynamic submarine electrical cable (DSEC) designed to sustain a maximum conductor temperature of 90 °C continuously. It is made up of 3 × 50 mm^2 copper conductors that are covered with a double wire armor to increase torsional stiffness due to dynamical application and to protect it from mechanical stress, floating debris, and friction caused by the cable touching the seabed. Figure 12 shows the high-voltage dynamic cable's complex hierarchical cross-sectional structure.

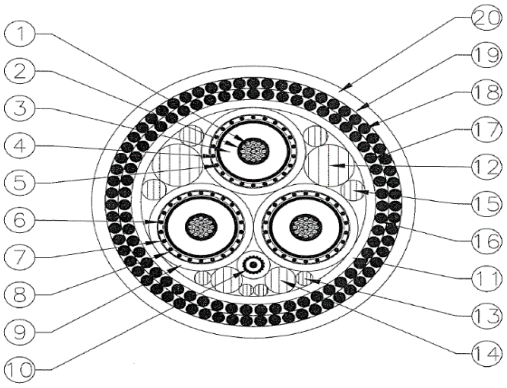

Item	Description
1	50 mm^2 copper conductor (19 strand construction, compliant with IEC 60228 class 2)
2	Polyethylene semiconducting conductor screen
3	Tree retardant cross linked polyethylene insulation
4	Polyethylene semiconducting insulation screen
5	Semiconducting waterblocking bedding tape
6	Diameter plain copper metallic screening wire
7	Copper equalisation tape
8	Non conducting waterblocking tape
9	High density polyethylene core sheath
10	Lose tube gel filled armored fiber tube
11	High density polyethylene bedding sheath
12,13,14 and 15	Polypropylene filler
16 and 18	Galvanized steel armor wire
17 and 19	Perfluoroelastomer (PFR) tape
20	High density polyethylene sheath

Figure 12. Cross section of a three phases DSEC.

Figure 13 shows a physical representation of the cable and its surroundings as a network of combined thermal resistances. All thermal resistances are calculated in accordance with IEC standard 60827-2 [18], where R_1 represents the thermal resistance per unit length between one conductor and the sheath (K.m.W^{-1}), R_2 represents the thermal resistance per unit length of the fillers and bedding under the armor (K.m.W^{-1}), R_3 represents the thermal resistance per unit length of the cable's external serving (K.m.W^{-1}), and R_4 represents the thermal resistance per unit length between the cable surface and the surrounding medium (K.m.W^{-1}), T_c (K) is the operating temperature of DSEC conductor, T_a (K) represents the ambient temperature, T_s (K) represents the sheath temperature, and T_0 (K) represents the outer serving temperature.

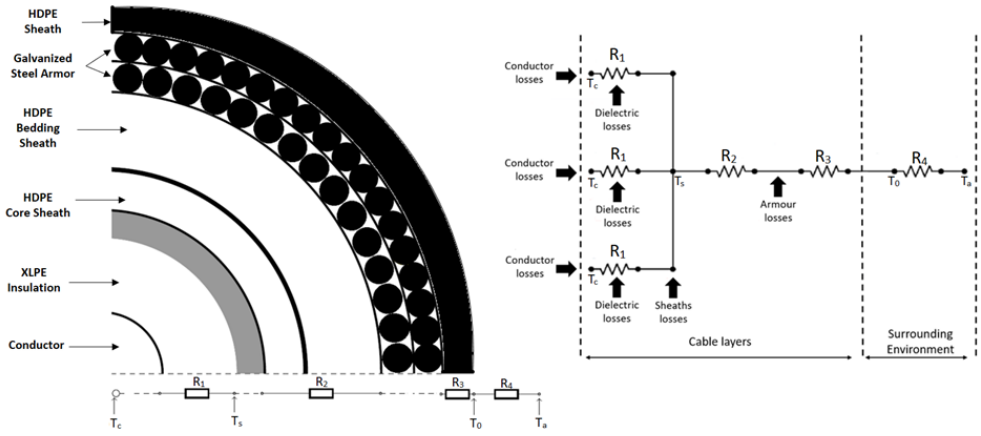

Figure 13. Network of thermal resistances representing steady state heat transfer in a three core submarine cable and its surrounding environment.

Using Ohm's law and the steady-state condition, which means that when the current flow through the cable is constant and the temperature of the cable is constant, the expression for the temperature rising above the surrounding temperature is represented in Equation (7).

$$\Delta\theta = (I^2 R_{AC} + 0.5W_d)R_1 + (I^2 R_{AC}(1+\lambda_1) + W_d)n\,R_2 + (I^2 R_{AC}(1+\lambda_1+\lambda_2) + W_d)n(R_3 + R_4) \quad (7)$$

Therefore, the maximum current that an AC cable can deliver is obtained as shown in Equation (8) [13]:

$$I = \left[\frac{\Delta\theta - W_d\,[0.5\,R_1 + n\,(R_2 + R_3 + R_4)]}{R_{AC}R_1 + nR_{AC}\,(1+\lambda_1)\,R_2 + nR_{AC}\,(1+\lambda_1+\lambda_2)\,(R_3+R_4)}\right]^{0.5} \quad (8)$$

Symbol	Material	Value
R_1	Thermal resistance between one conductor and the sheath per unit length (K.m.W^{-1})	0.587
R_2	Thermal resistance of the bedding between the sheath and the armor per unit length (K.m.W^{-1})	0.095
R_3	Thermal resistance of the cable's external serving per unit length (K.m.W^{-1})	0.035
R_4	Thermal resistance between the cable surface and the surrounding medium per unit length (K.m.W^{-1})	0.011
λ_1	Ratio of losses in the metal sheath to total losses in all conductors in that cable	0.05
λ_2	Ratio of losses in the armoring to total losses in all conductors in that cable.	0.112
R_{AC}	Alternating current resistance per unit conductor length at maximum operating temperature (Ω.km^{-1})	0.5
Wd	The dielectric loss per unit length of the insulation that surrounds the conductor (W.m^{-1})	0.074

where *I* represents the current flowing in a single conductor *(A)*, $\Delta\vartheta(K) = T_c - T_a$, n represents the number of copper conductors in the cable. λ_1 and λ_2 are calculated using IEC standard 60287-1 [13], where λ_1 is the ratio of losses in the metal sheath to total losses in all conductors in that cable, λ_2 is the ratio of losses in the armoring to total losses in all conductors in that cable. Also, R_{AC} and W_d are calculated using IEC standard 60287-2 [18], where R_{AC} denotes the alternating current resistance per unit length of the conductor at maximum operating temperature (Ω.m^{-1}) and W_d denotes the dielectric loss per unit length for the insulation surrounding the conductor (W.m^{-1}). The thermal resistances and the heat losses in the submarine power cable used for our calculations are shown in Table 8.

Table 8. Thermal resistances and heat losses in the submarine power cable.

* These resistances are calculated for 90 °C operating temperature and 20 °C ambient temperature.

3.2. Numerical Simulation of Temperature Field in a 2D DSEC

In this section, the thermal effect of mussels of various ages on the DSEC copper wire is investigated by predicting the temperature distribution within the cable using a two-dimensional steady-state thermal model computed using finite elements (COMSOL software) with heat conduction equation using a mesh with 2000 to 5000 nodes in the biofouling region and in the DSEC respectively.

As mentioned earlier, the DSEC is designed to support a maximum copper wire temperature of 90 °C. Therefore, for a maximum operating temperature of 90 °C and an ambient temperature of 20 °C, the permissible current rating (364 A) is calculated using Equation (8). The obtained current rating (364 A) is then imposed in the numerical method of DSEC 2D thermal modeling (COMSOL software). Moreover, with an external temperature of 20 °C, a convective heat transfer coefficient (247 $W.m^2.K^{-1}$) is applied to the outer layer of the DSEC; this convective heat transfer coefficient is calculated using the classic natural convection formula (Morgan's correlation). The steady-state temperature distribution in the cable is depicted in Figure 14. According to the results, the maximum conductor temperature calculated using a two-dimensional numerical thermal model is 90.15 °C, which is nearly equal to the maximum operating temperature of 90 °C. This means that the numerical approach is validated because the simulation code (COMSOL) produces the same temperature as the IEC-60827 standard. The numerical thermal model can then be used to investigate the thermal effect of biofouling colonization on the DSEC conductor temperature.

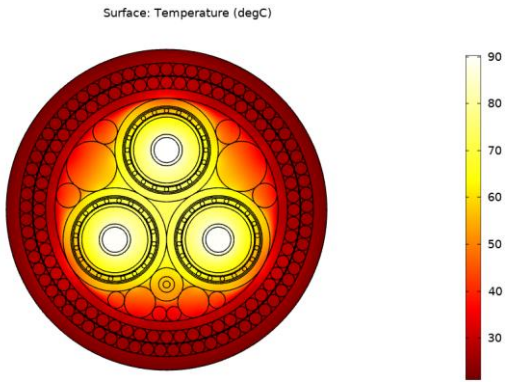

Figure 14. Simulation of the DSEC steady-state temperature distribution (°C) under rated load conditions.

The thermal effect of mussels on the DSEC conductor temperature is investigated by adding an extra layer around the cable in the COMSOL simulation (Figure 15). In these computations, the effective thermal conductivity of the external layer and the heat transfer coefficient of the water around the mussels of different ages are the ones measured in Section 2.2.3 (Tables 2 and 3). It should be noted that the thicknesses of mussel layers with different ages are implemented in the numerical simulation by defining the geometry of the mussel layer with the same thicknesses of mussel layers during thermal characterization in Section 2.2.2 (40 mm for juvenile, 60 mm for mix and 70 mm for adult mussels).

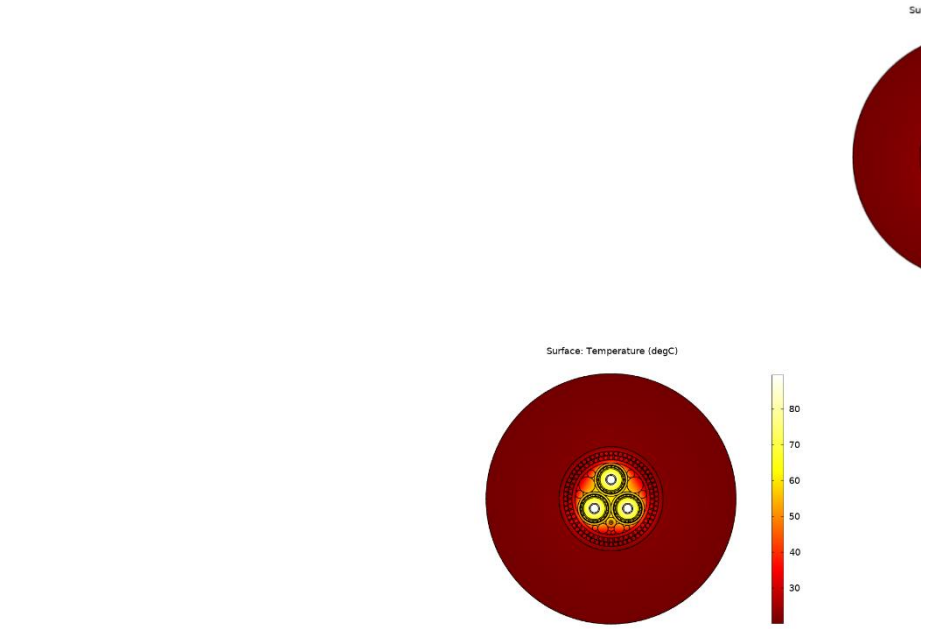

Figure 15. Steady-state temperature (°C) distribution for different ages of mussels (**a**) Juvenile, (**b**) Mix (**c**) Adult.

As shown in Figure 16, the DSEC conductor temperature T_c decreases with increasing mussel age: 91.3 °C (juvenile), 90.6 °C (mix), 89.6 °C (adult). Thus, juvenile mussels have the highest effect on the DSEC conductor temperature, because as previously described in Section 2.2.3, juvenile mussels have the greatest thermal resistance and thermal resistance decreases with the age of the mussels due to the increase in water porosity. Therefore, the colonization of juvenile and mix mussels on DSEC leads to conductor temperatures higher than the maximum operating temperature (90 °C); however, this is not the case for adult mussels.

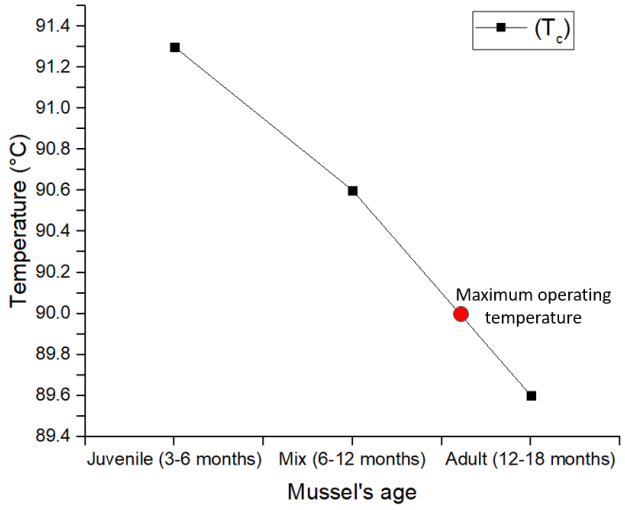

Figure 16. DSEC conductor temperature in function of mussel age.

This result appears to indicate that the temperature of the conductor decreases with mussel age and can be even lower than the temperature without mussels, which is used as a reference here. This observation must be moderated due to several aspects of our study: (i) the experiments and simulations are conducted with a single layer of mussels of roughly the same order of thickness. In

reality, as time passes from one season to the next, a new layer of mussels grows on top of the existing one. The water porosity and effective thermal conductivity will then evolve over time. This may cause the conductor to overheat. (ii) As previously stated, the value of effective thermal conductivity is related to natural convection in the porous medium composed of mussels. This natural convection effect is determined by the temperature difference across the mussel layer. The goal is to investigate the effect of mussel colonization on the copper conductor temperature of an electrical cable with a maximum operating temperature of 90 °C. In this case, we used the power calculated according to the IEC standard in our numerical simulations. Then, we imposed the measured effective thermal conductivity of the various mussel layers. The power values used in the experimental measurement differ from the power calculated using the IEC standard, which is used in the numerical simulations. This results in a difference in ΔT between experimental measurements and numerical simulations, as shown in Table 9. This disparity in ΔT values is expected because the power imposed in numerical simulation differs from the power imposed in experimental measurement, and effective thermal conductivity depends on ΔT. This difference affects the determination of the simulated temperature of the copper conductor. Therefore, in order to improve the accuracy of this temperature determination, the appropriate effective thermal conductivity of the mussels must be imposed in the numerical simulation. At this stage of our work, we don't have access to the variation of this thermal property with ΔT. This issue will be addressed in our next work.

Table 9. The temperature difference between the mussel layer's inner and outer radiuses.

Mussels Type	**ΔT (Measurement)**	**ΔT (COMSOL)**
	K	**K**
Juvenile	10	3.3
Mix (juvenile & adult)	4.2	2.4
Adult	4.8	1.7

ΔT is the temperature difference between the inner and outer radiuses of the mussel layer.

4. Conclusions

In this study, the thermal characterization of a mussel layer around a tube was carried out. The measurement of the thermal properties of this natural medium (biofouling) is rarely addressed in the marine energy literature. The experimental work was extremely difficult because we had to perform all experiments in 24 h in order to keep the mussels alive. In the uniform mussel colonization case, the thermal conductivity of different ages of mussels (juvenile, mix-juvenile and adult, and adult) as well as the heat transfer coefficient of the water around the mussels were measured. We have determined that juvenile mussels have the lowest effective thermal conductivity when compared to a mix of juvenile and adult mussels and adult mussels due to the water porosity effect. The effect of water porosity has been highlighted and illustrated using a glass beads medium, where it is demonstrated that the natural convection in the porous media significantly enhances the thermal conductivity of the glass porous media. Furthermore, the thermal risk on the DSEC is evaluated by estimating the temperature distribution within the electric cable covered with mussels of various ages and the type of colonization using a numerical code (COMSOL). Depending on the mussels' age and the corresponding global thermal resistance, the bio-colonization results in an overheating of the cable with juvenile and mix (juvenile and adult) mussels and a cooling down with the adult mussels. Those

measurements were carried out for a given thickness of the layer of mussels and do not take into account the evolution of bio-colonization over time (multi-layer effects). This aspect will be addressed in our future work. A new measurement and thermal characterization campaign for different ages of mussels colonized naturally on four tubes submerged in the Atlantic Ocean and the Mediterranean Sea is planned in the BIODYTHERM project, with thermal conductivities measured as a function of the temperature gradient (ΔT) through the mussel layer. Since measurements were performed in a range of ΔT over the mussel's layer between 4 K and 10 K in the present work, however, we expect some variation in the value of measured effective thermal conductivity with the ΔT. This effect will be investigated in our future measurements. This will allow us to carry out simulations with configurations closer to real experimental conditions.

Author Contributions:

Conceptualization, Z.M, B.G, F.S., A.M. and E.S.; methodology, Z.M, B.G, A.M. and F.S.; software, Z.M.; validation, Z.M., B.G., A.M. and F.S.; formal analysis, Z.M., B.G., A.M. and F.S.; investigation, Z.M., B.G., A.M. and F.S.; resources Z.M, B.G, F.S., A.M.; data curation, Z.M.; writing—original draft preparation, Z.M., B.G., A.M. and F.S; writing—review and editing, Z.M., B.G., A.M. and F.S; visualization, Z.M., B.G., A.M. and F.S; supervision, B.G., A.M. and F.S; project administration, A.M.; funding acquisition, F.S.

Funding: Region Pays de la Loire under the project BIODYTHERM(Effet de la BIOcolonisation des ombilicaux DYnamiques sur les échanges THERMiques) granted by WEAMEC; France Energies Marines and French National Research Agency (Project OMDYN-2: Dynamic umbilicals for floating marine renewable energies)

Institutional Review Board Statement: The study was conducted according to the guidelines of the Declaration of Helsinki, and approved by the Institutional Review Board (or Ethics Committee) of *LTeN & GeM.*

Informed Consent Statement: Informed consent was obtained from all subjects involved in the study.

Data Availability Statement: This study did not report any data.

Acknowledgments: This work was carried out within the framework of the BIODYTHERM project granted by WEAMEC, West Atlantic Marine Energy Community, and with funding from the Pays de la Loire Region. Also, It's a part of OMDYN-2 project: Dynamic Umbilicals for floating marine renewable energies granted by France Energies Marines and French National Research Agency.

Conflicts of Interest: The authors declare no conflict of interest

References

1. Wind Systems. Available online: https://www.windsystemsmag.com/the-advantages-of-floating-wind-turbines/ (accessed 10 April 2022).
2. American Geosciences Institute. Available online: https://www.americangeosciences.org/critical-issues/faq/what-are-advantages-and-disadvantages-offshore-wind-farms/ (accessed 5 May 2020).
3. Benifla, V.; Adam, F. Development of a Genetic Algorithm Code for the Design of Cylindrical Buoyancy Bodies for Floating Offshore Wind Turbine Substructures. *Energies* **2022**, *15*, 1181. https://doi.org/10.3390/en15031181.
4. Marini, M.; Baccoli, R.; Mastino, C.; Di Bella, A.; Bernardini, C.; Masullo, M. Assessment of the Noise Generated by Wind Turbines at Low Frequencies. *Energy Resour. Technol*. **2017**, *139*, 051215. https://doi.org/10.1115/1.4037088.
5. Yang, H.-S.; Alkhabbaz, A.; Edirisinghe, D.S.; Tongphong, W.; Lee, Y.-H. FOWT Stability Study According to Number of Columns Considering Amount of Materials Used. *Energies* **2022**, *15*, 1653. https://doi.org/10.3390/en15051653.
6. Weerheim, R. Development of Dynamic Power Cables for Commercial Floating Wind Farms. Master's Thesis, Delft University of Technology, Delft, The Netherlands, (12 November 2018)
7. Cruciani, M. *L'éolien Offshore Flottant dans sa Dimension Industrielle et Technologie. French.* Etudes de l'Ifri. Paris, France. (July 2019).
8. Sievers, M. Biofouling leads to reduced shell growth and flesh weight in the cultured mussel Mytilus galloprovincialis. *Biofouling* **2012**, *29*, 97–107. https://doi.org/10.1080/08927014.2012.749869.
9. Valdez, B.; Ramirez, J.; Eliezer, A.; Schorr, M.; Ramos, R.; Salinas, R. Corrosion assessment of infrastructure assets in coastal seas. *Mar. Eng. Tech.* **2016**, *15*, 124–134. https://doi.org/10.1080/20464177.2016.1247635.
10. Schoefs, F.; Tran, T.-B. Reliability Updating of Offshore Structures Subjected to Marine Growth. *Energies* **2022**, *15*, 414. https://doi.org/10.3390/en15020414.
11. Marty, A.; Berhault, C.; Damblans, G.; Facq, JV.; Gaurier, B.; Germain, G.; Soulard, T.; Schoefs, F. Experimental study of marine growth effect on the hydrodynamical behaviour of a submarine cable. *Appl. Oce. Res.* **2021**, *114*, 102810. https://doi.org/10.1016/j.apor.2021.102810.
12. Marty, A.; Schoefs, F.; Soulard, T.; Berhault, C.; Facq, J.-V.; Gaurier, B.; Germain, G. Effect of Roughness of Mussels on Cylinder Forces from a Realistic Shape Modelling. *Mar. Sci. Eng*. **2021**, *9*, 598. https://doi.org/10.3390/jmse9060598.
13. [IEC] The International Electroctechnical Comission. Electric cables—Calculation of the current rating—Current rating equations (100% load factor) and calculation of losses. *IEC 60287-1* 2014.
14. Fitridge, I. Ruinous resident: The hydroid Ectopleura crocea negatively affects suspended culture of the mussel Mytilus galloprovincialis. *Biofouling* **2013**, 29, 119–131. https://doi.org/10.1080/08927014.2012.752465.
15. Incropera, F.P.; Dewitt, B.P.; Bergman, T.L.; Lavine, A.S. *Fundamentals of Heat and Mass Transfer*, 6th ed.; John Wiley: Hoboken, New Jersey, USA, 2007.

16. Moffat, R. Describing the uncertainties in experimental results. *Exp. Therm and Fluid Sc.* **1988**, *1*, 3–17.

17. Maxwell, J.C. *A Treatise on Electricity and Magnetism*, 3rd ed.; Oxford University Press: Oxford, UK, 1982.

18. [IEC] The International Electroctechnical Comission. Electric cables—Calculation of the current rating, Thermal resistance—Calculation of thermal resistance. *IEC 60287-2* 2015.